Universitat de Lleida

Phenology and plant functional type dominance drive CO_2 exchange in seminatural grasslands in the Pyrenees

Abstract

Understanding the mechanisms underlying net ecosystem CO_2 exchange (NEE) in mountain grasslands is important to quantify their relevance in the global carbon budget. However, complex interactions between environmental variables and vegetation on NEE remain unclear; and there is lack of empirical data, especially from the high elevations and the Mediterranean region. A chamber-based survey of CO_2 exchange measurements was carried out in two climatically contrasted grasslands (montane *vs.* subalpine) of the Pyrenees; assessing the relative contribution of phenology and environmental variables on CO_2 exchange at seasonal scale, and the influence of plant functional type dominance (grasses, forbs and legumes) on NEE light response. Results show that phenology plays a crucial role as CO_2 exchange driver, suggesting a differential behaviour of the vegetation community depending on the environment. The subalpine grassland had a more delayed phenology compared to the montane, being more temperature than water constrained. However, temperature increased net CO_2 uptake at a higher rate in the subalpine than in the montane grassland. During the peak biomass, productivity (+74%) and net CO_2 uptake (NEE +48%) were higher in the subalpine grassland than in the montane grassland. The delayed phenology at the subalpine grassland reduced vegetation's sensitivity to summer dryness, and CO_2 exchange fluxes were less constrained by low soil water content. NEE light response suggested that legume dominated plots had higher net CO_2 uptake per unit of biomass than grasses. Detailed information on phenology and vegetation composition is essential to understand elevation and climatic differences on CO_2 exchange.

Introduction

Grasslands are the most widespread habitat in the world and provide crucial goods and services for human population, including animal feeding, climate regulation and carbon cycling (Hooper *et al.* 2005). Extensively managed mountain grasslands in particular, are some of the most species-rich ecosystems (Wilson *et al.* 2012), store about 100 t/ha of soil carbon (Sjögersten *et al.* 2011), and their net ecosystem exchange (NEE, Woodwell and Whittaker 1968) is mostly dominated by assimilation (Gilmanov *et al.* 2007; Soussana *et al.* 2007; Berninger *et al.* 2015).

However, there is still a lack of empirical data, mainly from the high elevations and from some regions, including the Mediterranean basin, in which climate change impacts are projected to be very severe (García-Ruiz *et al.* 2011). In the particular case of the Pyrenees, despite the few corresponding studies (Wohlfahrt *et al.* 2008a; Sjögersten *et al.* 2012; Berninger *et al.* 2015), NEE datasets are very limited, and knowing the particularities of these systems may provide some guidelines to adapt and mitigate climate change effects in this region.

Moreover, mountain grasslands are especially vulnerable to climate and land use changes (European Commission 2008) and mid- to long-term effects on the carbon budget still remain controversial (Wu *et al.* 2011), partly due to complex interactions between environmental variables and vegetation. Indeed, although the role of main environmental CO_2 exchange drivers, such as photosynthetically active radiation (Wohlfahrt *et al.* 2008b), temperature and soil moisture (Davidson & Janssens 2006; Albergel *et al.* 2010; Yvon-Durocher *et al.* 2012) has been widely assessed, how they interact with phenology and vegetation composition still needs deeper understanding.

Vegetation in mountain grasslands is highly dynamic, changing its structure and composition over time and space (Faurie *et al.* 1996; Giunta *et al.* 2009; Mitchell &

Bakker 2016), resulting in a variable patchy configuration of species (Schwinning & Parsons 1996), and generating differences in biogeochemical cycles and CO_2 exchange (Reich *et al.* 1997). While it is known that the aboveground living biomass directly takes- up (Wohlfahrt *et al.* 2008b; Nakano & Shinoda 2014) and releases CO_2 (Kardol *et al.* 2010; Thakur & Eisenhauer 2015), phenology and vegetation structure may be also determinant for the NEE. Indices of phenological development related to plant productivity, including total green biomass and normalized difference vegetation index (Gao *et al.* 2016; Zhou *et al.* 2016) have already been used to estimate gross primary production (GPP, Filippa *et al*. 2015) and ecosystem respiration (R_{eco}, Ryan & Law 2005).

However, when assessing mountain grasslands there are differences in phenological cycles between elevation belts (Liu *et al*. 2014; Leifeld *et al*. 2015), which may result in more complex vegetation-CO_2 exchange interactions than expected. In addition, there are other vegetation fractions, such as standing dead biomass (dead biomass attached to the plant) and litter (dead plant material, detached from the plant and laying on the soil surface), which are present in considerable amounts in grasslands, and whose specific role as CO_2 exchange drivers has been barely considered (Leitner *et al*. 2016; Gliksman *et al*. 2018).

On the other hand, vegetation composition has also been reported to drive CO_2 exchange fluxes (De Deyn *et al*. 2009; Metcalfe *et al*. 2011; Ribas *et al*. 2015). A common approximation to assess this vegetation-CO_2 exchange relationship is to separate plant species into plant functional types (PFT) that share a common response to an environmental factor, "response traits", and/or a common effect on ecosystem processes, "effect traits" (Lavorel & Garnier 2002). In the specific case of grasslands, species are often classified in grasses, non-legume forbs (hereafter "forbs") and legume

forbs (hereafter "legumes"), classification that is based on nitrogen and light (and therefore CO_2) acquisition and use (Tilman 1997; Symstad 2000; Díaz *et al*. 2007; defined as "guilds" in Sebastià 2007). Thus, legumes have the capacity to fix symbiotic nitrogen, while grasses have some advantages when competing for light as they are usually taller than legumes and forbs, and have erect high-density leaves that ensure good light penetration (Craine *et al.* 2001). However, there is still some uncertainty about how these PFT can differentially influence CO_2 exchange at plot scale .

Accordingly, in the present study we investigate the interaction between environmental variables and vegetation on CO_2 exchange fluxes, and more specifically we aim to: (1) compare the contribution of vegetation phenology and environmental variables in two climatically contrasted mountain grasslands in the Pyrenees; and (2) assess the influence of vegetation composition, in terms of the dominant PFT (forbs, grasses and legumes), on light response and therefore on NEE. For that purpose, we performed a survey of CO_2 exchange measurements with a non-steady state chamber, aboveground biomass sampling and environmental variables recording in two extensively managed mountain grasslands in the Pyrenees, located in the montane and subalpine elevation belts, respectively.

Material and methods

Study sites

The study sites were two grazed mountain grasslands in the south-eastern Pyrenees: La Bertolina (BERT), located in Pla de Busa (42° 05' N, 1° 39' E, 1276 m a. s. l.), and Castellar de n'Hug (CAST) in Plans del Ginebrar (42° 18' N, 2° 02' E, 1900 m a. s. l.). Both sites were characterized by a Mediterranean climate regime, with spring and

99   autumn precipitations and relatively high summer temperatures (Figure 1.A). However,

100 each grassland had its own specific climatic characteristics and phenological

101 particularities, respective to the given elevation belt.

102   BERT was a typical montane grassland, with mean annual temperature of 9 ºC

103 and mean annual precipitation of 870 mm (Figure 1.A). In BERT, vegetation started to

104 grow (Figure 1.C) as soon as soil water content (SWC, Figure 1.B) increased, and

105 senescence started (Figure 1.C) as soon as SWC dropped and summer temperatures

106 became high ($T_a \sim 18$ºC, Figure 1.B). On the other hand, CAST was a subalpine

107 grassland, with mean annual temperature of 5.1 ºC and mean annual precipitation of

108 1189 mm (Figure 1.A). CAST was more temperature limited, and vegetation did not

109 start to grow (Figure 1.C) until temperatures increased up-to $\geq$ 5ºC, irrespective of the

110 highest spring SWC, which coincided with the snowmelt period and cold temperatures

111 ($T_a \leq 5$ ºC). Senescence started later at CAST than at BERT, and progressed more

112 slowly (Figure 1.C), despite the low- mid summer SWC (Figure 1.B).

113   Vegetation composition at BERT was characteristic of a montane meso-

114 xerophytic grassland, and CAST was a mesic subalpine grassland. Both sites were

115 extensively grazed, by cattle at BERT, with an average stocking rate of 0.44 livestock

116 units (LSU)/ha, from May to November; and by cattle and sheep at CAST, with an

117 average stocking rate of 0.74 LSU/ha, from late June to November (according to the

118 corresponding site managers). The montane grassland (BERT) sustained a lower

119 livestock density, although during a longer time period (~3.1 LSU month/ha/yr). On the

120 contrary, the subalpine grassland (CAST) was highly productive during the summer and

121 sustained a higher livestock density, but during a shorter time (~4.4 LSU month/ha/yr).

122 Farmers' expectation of the carrying capacity was ~44% higher at CAST than at BERT.

123 Grazing calendar and stocking rates were provided by the farmers and later confirmed

124 during sampling visits. Soil at BERT was udic calciustept and at CAST was lithic

125 udorthent (FAO 1998).

126 *Sampling design*

127 Two sampling designs were established to achieve the aims of the current paper: a

128 seasonal and a diel sampling. The aim of the seasonal sampling was to record temporal

129 CO_2 variability over the growing season and its relationship with environmental

130 variables and vegetation phenology. The seasonal sampling was carried out from April

131 to December of 2012, at three-weekly intervals. Every sampling day, sampling points of

132 grassland patches (n = 10 at BERT and n = 8 at CAST) were systematically placed

133 within the footprint of the respective eddy covariance flux stations previously installed

134 at each site (Figure 2), which provided ancillary meteorological variables.

135 At each sampling point, complete CO_2 exchange measurements (NEE and

136 ecosystem respiration, R_{eco}, see CO_2 exchange flux calculations) were recorded twice

137 during daytime (08:00-16:30 UTC). After CO_2 exchange measurement, total

138 aboveground biomass was harvested at ground level. Total aboveground biomass was

139 separated into the different vegetation fractions: aboveground living biomass (AGLB),

140 standing dead biomass (SDB, dead biomass attached to the plant) and litter (dead plant

141 material, detached from the plant and on the soil surface) to characterize vegetation

142 phenological changes. Dry weight (DW, g/m^2) of all vegetation fractions was

143 determined after oven drying at 60 ºC until constant weight.

144 The aim of the diel sampling was to assess the effect of the dominant PFT on

145 NEE, via PFT-specific light response. A campaign of intensive CO_2 exchange

146 measurements was carried out at each site, coinciding with the peak biomass (end of

147 May at BERT, day of year (DOY) 150-152, and end of June at CAST, DOY 172-173),

148 to reduce the variability related to different phenological stages and/or environmental

149   conditions, and focusing on the effect of the PFT dominance. Sampling points were

150   selected to ensure the presence of patches with dominance of forbs (F-dominated),

151   grasses (G‑dominated) and legumes (L‑dominated), selecting three replicates for each

152   PFT (n = 9 in both sites). CO_2 exchange complete measurements (NEE and R_{eco}) were

153   done intensively during 48 h at BERT and 24 h at CAST, resulting in 75 complete CO_2

154   exchange measurements in BERT and 46 at CAST.

155   As in the seasonal sampling, total aboveground biomass was harvested after CO_2

156   exchange measurements, and processed in the same way. However, to verify that the

157   PFT dominance classification (F‑dominated, G‑dominated, L‑dominated) given in the

158   field was correct, the AGLB was separated into PFT (forbs, grasses and legumes) to

159   determine the fraction of each PFT, after oven drying at 60 ºC until constant weight.

160   Afterwards, the evenness index was calculated according to Kirwan *et al* (2007),

161   which has been defined as a measure of the distribution of the relative abundance of

162   each PFT or species, and lies between 0, for mono-specific plots, and 1 when all species

163   or PFT are equally represented (Kirwan *et al.* 2007). A cluster analysis (Ward's method)

164   was performed based on the PFT proportions and the evenness index, confirming the

165   PFT dominance classification given in the field. Plots G-dominated had generally very

166   low evenness and very high grass proportion, while F‑dominated and L-dominated

167   plots had higher values of evenness and the proportion of forbs and legumes, was not so

168   high (Figure S1).

169   *CO_2 exchange flux calculations*

170   CO_2 exchange measurements were carried out using a self-made non‑steady state

171   chamber, connected to an infrared gas analyser (LI-840, LI-COR, USA). Resulting CO_2

172   mixing ratios (ppm) were recorded at five seconds intervals by a laptop computer

173   connected to the gas analyser (Figure 3).

174   CO_2 exchange measurements were performed closing the chamber during 30

175   seconds in light conditions (NEE), and shading the chamber to create dark conditions

176   (R_{eco}). Gross primary production (GPP) was estimated as the sum of both fluxes. Prior

177   to flux calculation, mixing ratios were converted to molar densities (in mol/m^3, termed

178   as concentration in what follows) using the ideal gas law. Afterwards, CO_2 fluxes were

179   calculated based on the concentration change, following the mass balance equation

180   (Equation 1, Altimir *et al.* 2002):

$$CO_2 flux = q \, \frac{Ct - Ca}{A} + \frac{V}{A} \frac{dC}{dt}$$

181   (Equation 1)

182   Here q is the air flow rate (1.67 10^{-5} m^3/s, which is 1 litres/min), C_a the

183   atmospheric CO_2 concentration, C_t the CO_2 concentration inside the chamber at time t

184   (s), V the chamber volume (0.019 m^3), A the sampling surface (0.049 m^2) and (dC/dt)

185   the first derivative of the CO_2 concentration in relation to time (mol m^3/s). Fluxes from

186   the atmosphere to the biosphere were considered negative, and from the biosphere to the

187   atmosphere positive, according the micrometeorological sign convention.

188   Finally, data quality was checked based on the flux detection limit, calculated

189   from the standard deviation of the ambient concentration observed over the measuring

190   time, and on linearity (R^2) of the concentration change during the chamber closure.

191   Fluxes with an adjusted $R^2 < 0.8$ and/or below the detection limit were excluded from

192   further analysis (Debrouk *et al.* 2018).

193   In addition, the eddy covariance flux stations previously installed at each site

194   provided 30 min averaged meteorological data used in the site description (see Study

195   sites section) and CO_2 exchange modelling (see Data analysis section): air temperature

196   (T_a, HMP45C, Vaisala Inc, Helsinki, Finland); volumetric soil water content at 5 cm

197 depth (SWC, CS616, Campbell Scientific, Logan UT, USA); photosynthetically active

198 radiation (PAR, SKP215, Skye Instruments Ltd, Powys, UK); and normalized difference

199 vegetation index, calculated as NDVI = (NIR – Red) / (NIR + Red), where "Red" and

200 "NIR" are the spectral reflectance measurements acquired in the red and near-infrared

201 regions, respectively.

202

203 *Data analysis*

204 *Seasonal CO_2 dynamics*

205 All data analyses were performed using the R software (R core Team, 2015). To

206 describe seasonal CO_2 dynamics, average daytime CO_2 exchange fluxes were calculated

207 using data obtained between 8:00 and 16:30 UTM. To investigate the influence of

208 phenology and environmental variables on CO_2 exchange fluxes in the two climatically

209 contrasted grasslands, linear models were run with the given CO_2 flux (NEE, GPP or

210 R_{eco}), as function of vegetation fractions (AGLB as the Aboveground living biomass,

211 SDB as Standing dead biomass and litter) as a proxy of phenological changes, and

212 abiotic variables (T_a, SWC , PAR), in interaction with site (Equation 2). The inclusion

213 of "site" into the model incorporated the variability due to each specific grassland do

214 not assumed by the rest of explanatory variables, such as management for instance.

215 $CO_2 flux = Site(\beta_{AGLB}AGLB + \beta_{SDB}SDB + \beta_{Litter}Litter + \beta_{Ta}T_a + \beta_{SWC}SWC)$

216 (Equation 2)

217 Collinearity among variables was tested by the variance inflation factors (VIF)

218 tests, using the vif function, car package (Fox & Weisberg 2011). Collinearities between

219 variables were found to be not relevant (VIF < 5, Zuur *et al*. 2007). Final models were

220 selected by a stepwise procedure based on the Akaike information criterion (AIC) using

221   the stepAIC function, MASS package (Venables and Ripley 2002). The relative

222   importance of each predictive variable was determined by the calc.relimp function,

223   relaimpo package (Groemping 2006).

224   *Plant functional type dominance on NEE light response*

225   To assess the influence of PFT dominance on NEE, the NEE *vs.* PAR relationship was

226   modelled using a logistic sigmoid light response function (Equation 3, Moffat 2012).

$$NEE = -\,2GPP_{sat}\left(-\,0.5 + \frac{1}{1 + e^{\dfrac{-\,2\alpha PAR}{GPP_{sat}}}}\right) + R_{ecoday}$$

227   (Equation 3)

228   Here GPP_{sat} is the asymptotic gross primary production, α is the apparent

229   quantum yield, defined as the initial slope of the light-response curve, and $R_{eco,day}$ the

230   average daytime ecosystem respiration (Equation 3). Two variants of NEE *vs.* PAR

231   relationships were fitted: (1) using flux densities per grassland ground area (NEE, μmol

232    $CO_2/m^2/s$) and (2) using NEE normalized by aboveground living biomass

233   (NEE_{AGLB}, μmol $CO_2/g/s$).

234   Afterwards, the PFT dominance effect was tested on light response parameters in

235   both cases, using nonlinear mixed- effects models (Pinheiro & Bates 2000), by the nlme

236   function of the nlme package (Pinheiro *et al.* 2015). For that purpose, null models in

237   each case (NEE ~ PAR, Model 1.1, and NEE_{AGLB} ~ PAR, Model 2.1) were performed,

238   with site as random factor and light response parameters (Equation 3: α, GPP_{sat} and

239    $R_{eco,day}$) as fixed effects. Afterwards, corresponding models with PFT dominance as

240   covariates of the parameters, α, GPP_{sat} and $R_{eco,day}$ (Model 1.2 and Model 2.2) were also

241 run. Null models and models including PFT dominance as covariates were compared by

242 an analysis of variance (ANOVA).

243

244 **Results**

245 *Seasonal CO_2 flux dynamics in montane and subalpine grasslands*

246 Mean daytime NEE was mostly dominated by assimilation at both sites, ranging from

247 -2 ± 1 to -10 ± 2 µmol $CO_2/m^2/s$ at BERT, and from 2 ± 1 to -20 ± 3 µmol $CO_2/m^2/s$ at

248 CAST. Mean daytime GPP showed the strongest seasonal pattern and the highest

249 differences between sites, ranging from -5 ± 1 to -20 ± 2 µmol $CO_2/m^2/s$ at BERT and

250 form -6 ± 1 to -32 ± 2 µmol $CO_2/m^2/s$ at CAST. Finally, mean daytime R_{eco} ranged

251 from 3.0 ± 0.4 to 10 ± 1 µmol $CO_2/m^2/s$ at BERT and from 3.1 ± 0.5 to 15 ± 5 µmol

252 $CO_2/m^2/s$ at CAST (Figure 4.A).

253   CO_2 exchange seasonal patterns (Figure 4.A), evolved according to

254 environmental conditions (Figure 4.B) and phenology (Figure 4.C). The modelling

255 showed that NEE was mainly driven by AGLB (Figure 5), increasing net CO_2 uptake —

256 more negative NEE — with increasing AGLB (Table 1); while net CO_2 uptake decreased

257 with increasing SDB and litter (Table 1).

258   Moreover, there were some interactions between site and environmental

259 conditions (Table 1 and Figure 5). Net CO_2 uptake was a priori lower at CAST than at

260 BERT (less negative NEE, site effect, Table 1), and the AGLB was proportionally

261 taking-up CO_2 at lower rates at CAST than at BERT (site x AGLB, Table 1). However,

262 net CO_2 uptake increased with temperature at a higher rate at CAST than at BERT (site

263 x T_a effect, Table 1).

264   GPP behaved similarly to NEE. GPP was mainly driven by AGLB (Figure 5),

265   increasing the gross uptake — more negative GPP — with increasing AGLB, and

266   decreasing the gross uptake with SDB (Table 1). Gross uptake in addition increased

267   with increasing temperature and SWC (Table 1). GPP presented the same interactions

268   between site, environmental variables and vegetation as NEE did (Table 1). Finally, R_{eco}

269   was also mainly driven by AGLB (Figure 5), increasing emissions with AGLB,

270   followed by temperature, and SWC (Table 1).

271   *Plant functional type dominance on NEE light response*

272   CO_2 exchange fluxes recorded during the intensive diel campaign confirmed that NEE

273   was mainly driven by PAR at a diel timescale (Figure 6). The logistic sigmoid light

274   response function (Equation 3) explained 69% of the variability, when assessing NEE

275   per grassland ground area (Model 1.1, Table 2).

276   The inclusion of PFT dominance as covariates of the light response function

277   parameters (α, GPP_{sat} and $R_{eco,day}$), was not significant when assessing NEE per

278   grassland ground area (Model 1.2, Table 2). However, the logistic sigmoid adjustment

279   per site and per PFT dominance suggested that there were differences between PFT

280   when assessing the NEE per unit of AGLB (NEE_{AGLB}, Figure 6.B). Accordingly, when

281   assessing the $NEE_{AGLB} \sim$ PAR relationship, there were significant differences between

282   the null model and the model that included PFT dominance as covariate of the

283   parameters (ANOVA Model 2.1 *vs*. Model 2.2, Table 2), which also increased the

284   explained variability, from 0.66 to 0.72 (R^2 Model 2.1 *vs*. Model 2.2, Table 2).

285   Differences among PFT in the NEE_{AGLB} were mainly driven by differences in the GPP_{sat},

286   G-dominated plots having significantly lower GPP_{sat} than L-dominated plots

287   (Model 2.2, Table 2).

Discussion

Differential contributions of phenology and environmental variables on CO_2 seasonal dynamics between elevation belts

Contextualizing recorded CO_2 exchange fluxes (Figure 4.A), they were higher than in other seminatural grasslands in the Pyrenees previously reported (Gilmanov *et al.* 2007, 2010; Wohlfahrt *et al.* 2008a; Sjögersten *et al.* 2012).

For instance, Gilmanov et al. (2007) reported in Alinyà, a montane grassland (1770 m a.s.l) that might be climatically comparable to BERT, maximum daily aggregated GPP of −25.7 g CO_2/m^2/d. Whereas in BERT, considering the light response function (Equation 3), the estimates of the parameters subtracted from the NEE_{AGLB} ~ PAR relationship (Table 2, Model 2.1), and the AGLB sampled during the peak biomass (190 ± 21 g DW/m^2, DOY 150, Figure 4.C), maximum daily aggregated GPP can be estimated ≈ −31 g CO_2/m^2/d. Such difference may well be because there are important vegetation differences between both sites, with a maximum productivity at Alinyà around 131 ± 12 g DW/m^2 (unpublished data), while at BERT it is roughly a 45% higher (190 ± 21 g DW/m^2), although other factors, as for instance soil differences — soil at Alinyà is a lithic cryrendoll (Gilmanov *et al.* 2007), while the soil at BERT is a udic calciustept — may also be influencing.

Another example is the CO_2 exchange fluxes reported by Sjögersten *et al*. (2012) in a subalpine grassland of the southeaster Pyrenees, very close to our subalpine site CAST. They reported maximum NEE values of −0.7 ± 0.8 µmol CO_2/m^2/s in June, while our NEE in a similar date (DOY 172, −20 ± 3 µmol CO_2/m^2/s, Figure 4.A) amply exceed this value. Such a huge difference is only realistic if it is the result of a large difference in AGLB between both grasslands, possibly in combination with different phenological development stages and grazing pressure. Sjögersten *et al*. (2012) reported

313   in June an AGLB of 107 ± 15 g DW/m^2, while in our site CAST we had 330 ± 40

314   g DW/m^2 in late June (+210%, DOY 172, Figure 4.C), reaching the peak biomass

315   around that date. Indeed, the AGLB reported by Sjögersten *et al.* (2012) in June is more

316   similar to our value in late May (DOY 146, 116 ± 33 g DW/m^2, Figure 4.C). These

317   differences reveal how dynamic those grasslands are, and exemplify the need for a

318   better understanding of CO_2 drivers in mountain ecosystems to perform accurate

319   predictions and upscaling.

320   In line with this dynamism, our results emphasize the role that phenology plays

321   as an important factor influencing CO_2 exchange fluxes. The well-known effect of

322   AGLB as CO_2 exchange driver was clear, but the relevance of other vegetation fractions,

323   including SDB and litter, which lowered the gross and net CO_2 uptake capacity of the

324   ecosystem (Table 1 and Figure 5) was important.

325   Moreover, there were interesting interactions between site, phenology and

326   environmental variables. On one hand, the AGLB at the subalpine grassland, CAST,

327   was proportionally taking-up CO_2 at lower rates than at the montane grassland BERT;

328   resulting in proportionally lower rates of NEE per unit of AGLB (site x AGLB effect on

329   NEE, Table 1). This suggests that environmental conditions were more constraining in

330   CAST than at BERT, and vegetation at CAST could proportionally photosynthesize at

331   lower rates than at BERT. However, although CAST was probably more temperature

332   limited, the gross and net CO_2 uptake capacity increased more markedly in CAST than

333   at BERT as soon as temperatures increased (site x T_a effect on NEE and GPP, Table 1).

334   Accordingly, some ecosystem functions, including biomass production and CO_2

335   exchange, in high elevation mountain grasslands have been reported to be more

336   temperature-limited than water-limited (Sebastià 2007), being mostly constrained to the

337   warm months. Thus, the pronounced gross and net CO_2 uptake with vegetation

338   development at CAST (Figure 4), is in line with the fact that in the Mediterranean

339   region high‑elevation grasslands are generally highly productive during the summer,

340   while montane grasslands have a longer growing season but less productive

341   (García‑González, 2008). In fact, these phenological differences describe their

342   managing use.

343   On the other hand, there were important site differences in the way that SWC

344   drove GPP and R_{eco} (Figure 4), partly related to phenological differences between both

345   elevations and vegetation development strategies. SWC enhanced both gross CO_2

346   uptake and release fluxes (Table 1), in agreement with earlier works (Law *et al.* 2002;

347   Flanagan & Johnson 2005; Davidson & Janssens 2006; Bahn *et al.* 2008; Imer *et al.*

348   2013). However, when the SWC dropped, CO_2 exchange fluxes diminished especially at

349   BERT, while that diminishment at CAST was not so pronounced. Hence, although the

350   SWC during the peak-biomass was clearly lower at CAST than at BERT (Figure 4.B,

351   SWC below 10% indicates a dry period), the low SWC did not cause an immediate

352   decrease of the CO_2 exchange fluxes at CAST (Figure 4.A).

353   This may well be because CAST had high SWC during the spring, which

354   allowed the development of the vegetation, once the temperature increased (Figure 4).

355   The well‑developed AGLB was able to cope with the SWC deficit during the summer

356   drought, and GPP and R_{eco} did not decrease at CAST as much as at BERT. This suggests

357   that BERT was probably more water-limited than CAST, in agreement with some

358   studies that have highlighted that summer drought effects on productivity (Gilgen &

359   Buchmann 2009) and CO_2 assimilation (Bollig & Feller 2014) may be more intense at

360   sites with lower annual precipitation, as is the case of BERT in comparison to CAST.

361   Accordingly, vegetation may be adopting different development strategies

362   between sites. Plants at CAST may be taking a "water spending strategy" (Leitinger *et*

363   *al.* 2015), meaning that some of the typical grassland species may not regulate the

364   stomatal conductance until the SWC approaches the wilting point under occasional

365   droughts (Brilli *et al.* 2011). However, it must be considered that long term changes in

366   water availability would finally lead to shifts in vegetation composition towards more

367   opportunistic species in perennial alpine and subalpine grasslands (Sebastià 2007;

368   Debouk *et al.* 2015).

369   Also, CAST has a less stony soil, which allows the development of a more

370   complex radicular system (mean belowground biomass in the first 20 cm at the peak

371   biomass stage in 2012: BERT, 730 and CAST, 3158 g DW/m^2, unpublished data), which

372   could be offsetting the superficial SWC deficit.

373   Ultimately, the inclusion of site could be acting as a proxy of the intrinsic

374   characteristics of each altitudinal belt (montane *vs.* subalpine), including information of

375   complex interactions between biotic and abiotic variables, as well as current and past

376   management practices (Leifeld *et al.* 2015).

377   Finally, AGLB was also an important driver of R_{eco} (Table 1 and Figure 5),

378   indicating that CO_2 release was most likely dominated by the autotrophic than by the

379   heterotrophic component of R_{eco}. In agreement, it has been reported that the magnitude

380   of R_{eco} components changes considerably over the year in grassland ecosystems, and the

381   autotrophic respiration reaches its maximum during the growing season (Gomez-

382   Casanovas *et al.* 2012).

383

384   *Plant functional type dominance on NEE light response*

385   PFT dominance influenced on NEE light response, when accounting for NEE_{AGLB}

386   (Model 2.2, Table 2). Grass dominated (G- dominated) plots had lower GPP_{sat}, than

387   plots dominated by legumes. This is in agreement with previous studies that have

388   reported that legumes yield higher CO_2 exchange rates than forbs and grasses, per unit

389   of biomass (Reich *et al.* 2003). Such differences in CO_2 exchange rates between PFT

390   dominance groups are most likely related to identity effects regarding the

391   ecophysiological characteristics of each PFT. Legumes have the ability to fix

392   atmospheric nitrogen (e.g. Reich *et al.* 2003, 1997) and have higher leaf nitrogen

393   content, which results in higher photosynthetic capacity and CO_2 uptake (Busch, Sage &

394   Farquhar 2018; Lee, Reich & Tjoelker 2003; Reich, Ellsworth & Walters 1998; Reich *et*

395   *al*. 1997). In addition, legumes have higher specific leaf area than grasses, a trait that

396   has been related to increased photosynthesis rates (Reich *et al.* 1998).

397   However, L-dominated plots tended to have lower AGLB than G-dominated and

398   F-dominated plots (Figure S2), and although G-dominated plots had lower GPP_{sat},

399   resulting in lower NEE_{AGLB} than L-dominated plots (Figure 6.B), their higher biomass

400   offset this difference at grassland ground scale (Model 1.2, Table 2). In this regard,

401   previous studies showed that different PFT have different strategies to produce and

402   maintain their biomass and access resources (Craine *et al.* 2002). Legumes access

403   nitrogen to avoid nutrient limitation and produce high-nitrogen biomass, while grasses

404   and forbs produce low-nitrogen biomass. Low-nitrogen species, especially grasses,

405   have lower rates of physiological activity but generate dense and long-lived tissues that

406   result in more biomass in the long term compared to high-nitrogen species, as is the

407   case of legumes (Craine *et al.* 2002). Moreover, symbiotic fixation of atmospheric

408   nitrogen by legumes requires additional energy in comparison to nitrogen acquisition

409   from the soil (Postgate 1998; Minchin & Witty 2005), causing more investment of

410   photosynthates in the nitrogen fixation processes.

411   In addition, apart from the effects referable to the identity effects of each PFT,

412   possible interactions between PFT must be considered. L-dominated plots had higher

413   evenness than G-dominated plots (Figure S1), meaning that L-dominated plots had

414   higher functional diversity. Hence, functional diversity and PFT interactions may be

415   producing an enhancement of the CO_2 exchange per unit of biomass in addition to the

416   rates of each single PFT. This would be in agreement with the "complementarity

417   hypothesis", which postulates that trait dissimilarity among species or PFT maximizes

418   resource use strategies and ecosystem functioning (Tilman *et al.* 1997). Several studies

419   have reported diversity and compositional effects, mainly due to grasses-legumes

420   interactions on several ecosystem functions, including CO_2 exchange, yield and/or

421   nitrogen availability (Nyfeler *et al.* 2009, 2011; Finn *et al.* 2013; Ribas *et al.* 2015). For

422   instance, Ribas *et al.* (2015) found the highest CO_2 respiration rates in plots dominated

423   by legumes with a certain proportion of grasses, and a positive effect of evenness on

424   respiration, verifying and disaggregating a coupled effect of the dominant PFT from

425   PFT interaction (evenness) effects.

426   In our study case, dominance and interaction effects cannot be disentangled, but

427   certainly PFT composition was influencing NEE_{AGLB} (Model 2.2, Table 2), via

428   PFT-specific light response differences, in seminatural mountain grasslands.

429

430   **Conclusions**

431   Phenology plays an important role as CO_2 exchange driver at seasonal scale, driving

432   differences between elevation belts (montane *vs.* subalpine). Although the subalpine

433   grassland (CAST) had a later vegetation development, CAST was clearly more

434   productive (AGLB ~ +74%) than the montane grassland (BERT) during the peak

435   biomass stage, and yielded higher NEE values (NEE ~ +48%). Thus, at least in

436   mountain environments, detailed information on phenology is key to understand the *a*

437   *priori* counterintuitive finding that a high-elevation grassland (CAST) is more

438   productive than a comparable grassland at the montane elevation (BERT), with a longer

439   growing season and warmer summer temperature. There were elevation differences in

440   the way that environmental variables and phenology mediated CO_2 exchange fluxes.

441   Although CAST was more temperature constrained, temperature enhanced gross and net

442   CO_2 uptake at higher rates at CAST than at BERT. Also, both grasslands experienced a

443   pronounced summer dry period, which substantially reduced productivity at the lower

444   elevation, from which only a minor recovery could be observed in autumn. However,

445   the delayed phenology at the subalpine grassland reduced vegetation's sensitivity to

446   summer dryness, which did not experience a reduction in CO_2 exchange, even though

447   the low SWC.

448   Moreover, vegetation composition, in terms of PFT, influenced on the CO_2

449   exchange. Legume dominated plots presented higher NEE rates than grass dominated

450   plots per unit of aboveground living biomass; with higher GPP_{sat} than grass dominated

451   plots. Overall, a deeper knowledge of phenology and vegetation ecophysiological

452   responses under different climatic conditions is key to upscale CO_2 exchange fluxes in a

453   seasonal and inter-annual scale in seminatural mountain grasslands.

454

Conflicts of Interest

467   The authors declare there are no conflicts of interest.

468

Ethical Standards

470   Not applicable.

References

Albergel C, Calvet J-C, Gibelin A-L, Lafont S, Roujean J-L, Berne C, Traullé O and Fritz N (2010) Observed and modelled ecosystem respiration and gross primary production of a grassland in southwestern France. *Biogeosciences*, **7**, 1657–1668.

Altimir N, Vesala T, Keronen P, Kulmala M and Hari P (2002) Methodology for direct field measurements of ozone flux to foliage with shoot chambers. *Atmospheric Environment*, **36**, 19–29. (2012) *Eddy Covariance. A Practical Guide to Measurement and Data Analysis* (Eds M. Aubinet, T. Vesala, & D. Papale). London and New York: Springer Netherlands.

Bahn M, Rodeghiero M, Anderson-Dunn M, Dore S, Gimeno C, Drösler M, Williams M, Ammann C, Berninger F, Flechard C, Jones S, Balzarolo M, Kumar S, Newesely C, Priwitzer T, Raschi A, Siegwolf R, Susiluoto S, Tenhunen J, Wohlfahrt G and Cernusca A (2008) Soil respiration in European grasslands in relation to climate and assimilate supply. *Ecosystems*, **11**, 1352–1367.

Berninger F, Susiluoto S, Gianelle D, Bahn M, Wohlfahrt G, Sutton M, Garcia-Pausas J, Gimeno C, Sanz MJ, Dore S, Rogiers N, Furger M, Balzarolo M, Sebastià MT and Tenhunen J (2015) Management and site effects on carbon balances of European mountain meadows and rangelands. *Boreal Environment Research*, **20**, 748–760.

Bollig C and Feller U (2014) Impacts of drought stress on water relations and carbon assimilation in grassland species at different altitudes. *Agriculture, Ecosystems and Environment*, **188**, 212–220.

Brilli F, Hörtnagl L, Hammerle A, Haslwanter A, Hansel A, Loreto F and

495 **Wohlfahrt G** (2011) Leaf and ecosystem response to soil water availability in
496 mountain grasslands. *Agricultural and Forest Meteorology*, **151**, 1731–1740.

497 **Busch FA**, **Sage RF** and **Farquhar GD** (2018) Plants increase CO_2 uptake by
498 assimilating nitrogen via the photorespiratory pathway. *Nature Plants*, **4**, 46–54.

499 **Craine JM**, **Froehle J**, **Tilman DG**, **Wedin DA** and **Chapin FS** (2001) The
500 relationships among root and leaf traits of 76 grassland species and relative
501 abundance along fertility and disturbance gradients. *Oikos*, **93**, 274–285.

502 **Craine JM**, **Tilman D**, **Wedin D**, **Reich P**, **Tjoelker M** and **Knops J** (2002)
503 Functional traits, productivity and effects on nitrogen cycling of 33 grassland
504 species. *Functional Ecology*, **16**, 563–574.

505 **Davidson EA** and **Janssens IA** (2006) Temperature sensitivity of soil carbon
506 decomposition and feedbacks to climate change. *Nature*, **440**, 165–173.

507 **Davidson EA**, **Savage K**, **Verchot L V** and **Navarro R** (2002) Minimizing artifacts
508 and biases in chamber-based measurements of soil respiration. *Agricultural and*
509 *Forest Meteorology*, **113**, 21–37.

510 **Debouk H**, **Altimir N** and **Sebastià MT** (2018) Maximizing the information obtained
511 from chamber-based greenhouse gas exchange measurements in remote areas.
512 *MethodsX*, **5**, 973–983.

513 **Debouk H**, **De Bello F** and **Sebastia MT** (2015) Functional trait changes, productivity
514 shifts and vegetation stability in mountain grasslands during a short-term warming.
515 *PLoS ONE*, **10**, 1–17.

516 **De Deyn GB.**, **Quirk H**, **Yi Z**, **Oakley S**, **Ostle NJ** and **Bardgett RD** (2009)
517 Vegetation composition promotes carbon and nitrogen storage in model grassland
518 communities of contrasting soil fertility. *Journal of Ecology*, **97**, 864–875.

519   **Díaz S**, **Lavorel S**, **McIntyre S**, **Falczuk V**, **Casanoves F**, **Milchunas DG**, **Skarpek**
520   **C**, **Ruschk G**, **Sternberg M**, **Noy-Meir I**, **Landsberg J**, **Zhang W**, **Clark H** and
521   **Campbell BD** (2007) Plant trait responses to grazing – a global synthesis. *Global*
522   *Change Biology*, **13**, 313–341.

523   **FAO** (1998) *World Reference Base for Soil Resources*. Rome.

524   **Faurie O**, **Soussana JF** and **Sinoquet H** (1996) Radiation Interception, Partitioning
525   and Use in Grass-Clover Mixtures. *Annals of Botany*, **77**, 35–45.

526   **Fick SE** and **Hijmans RJ** (2017) WorldClim 2: new 1-km spatial resolution climate
527   surfaces for global land areas. *International Journal of Climatology*, **37**, 4302–
528   4315.

529   **Filippa G**, **Cremonese E**, **Galvagno M**, **Migliavacca M**, **Morra di Cella U**, **Petey M**
530   and **Siniscalco C** (2015) Five years of phenological monitoring in a mountain
531   grassland: inter-annual patterns and evaluation of the sampling protocol.
532   *International Journal of Biometeorology*, **59**, 1927–1937.

533   **Finn JA**, **Kirwan L**, **Connolly J**, **Sebastià MT**, **Helgadottir A**, **Baadshaug OH**,
534   **Bélanger G**, **Black A**, **Brophy C**, **Collins RP**, **Čop J**, **Dalmannsdóttir S**,
535   **Delgado I**, **Elgersma A**, **Fothergill M**, **Frankow-Lindberg BE**, **Ghesquiere A**,
536   **Golinska B**, **Golinski P**, **Grieu P**, **Gustavsson A-M**, **Höglind M**, **Huguenin-Elie**
537   **O**, **Jørgensen M**, **Kadziuliene Z**, **Kurki P**, **Llurba R**, **Lunnan T**, **Porqueddu C**,
538   **Suter M**, **Thumm U** and **Lüscher A** (2013) Ecosystem function enhanced by
539   combining four functional types of plant species in intensively managed grassland
540   mixtures: a 3-year continental-scale field experiment. *Journal of Applied Ecology*,
541   **50**, 365–375.

542   **Flanagan LB** and **Johnson BG** (2005) Interacting effects of temperature, soil moisture

543   and plant biomass production on ecosystem respiration in a northern temperate

544   grassland. *Agricultural and Forest Meteorology*, **130**, 237–253.

545   **Fox J** and **Weisberg S** (2011) *An R Companion to Applied Regression. Second Edition*,

546   Second. Thousand Oaks, CA: Sage.

547   **Gao Q**, **Zhu W**, **Schwartz MW**, **Ganjurjav H** and **Wan Y** (2016) Climatic change

548   controls productivity variation in global grasslands. *Scientific Reports*, **6**, 1–10.

549   **García-González R** (2008) *Management of Natura 2000 Habitats. Alpine and*

550   *Subalpine Calcareous Grasslands 6170*.

551   **García-Ruiz JM**, **López-Moreno II**, **Vicente-Serrano SM**, **Lasanta-Martínez T** and

552   **Beguería S** (2011) Mediterranean water resources in a global change scenario.

553   *Earth-Science Reviews*, **105**, 121–139.

554   **Gilgen AK** and **Buchmann N** (2009) Response of temperate grasslands at different

555   altitudes to simulated summer drought differed but scaled with annual precipitation.

556   *Biogeosciences*, **6**, 2525–2539.

557   **Gilmanov TG**, **Aires L**, **Barcza Z**, **Baron VS**, **Belelli L**, **Beringer J**, **Billesbach D**,

558   **Bonal D**, **Bradford J**, **Ceschia E**, **Cook D**, **Corradi C**, **Frank A**, **Gianelle D**,

559   **Gimeno C**, **Gruenwald T**, **Guo H**, **Hanan N**, **Haszpra L**, **Heilman J**, **Jacobs A**,

560   **Jones MB**, **Johnson DA**, **Kiely G**, **Li S**, **Magliulo V**, **Moors E**, **Nagy Z**, **Nasyrov**

561   **M**, **Owensby C**, **Pinter K**, **Pio C**, **Reichstein M**, **Sanz MJ**, **Scott R**, **Soussana JF**,

562   **Stoy PC**, **Svejcar T**, **Tuba Z** and **Zhou G** (2010) Productivity, Respiration, and

563   Light-Response Parameters of World Grassland and Agroecosystems Derived

564   From Flux-Tower Measurements. *Rangeland Ecology Management*, **63**, 16–39.

565   **Gilmanov TG**, **Soussana JF**, **Aires L**, **Allard V**, **Ammann C**, **Balzarolo M**, **Barcza**

566   **Z**, **Bernhofer C**, **Campbell CL**, **Cernusca A**, **Cescatti A**, **Clifton-Brown J**,

567   **Dirks BOM, Dore S, Eugster W, Fuhrer J, Gimeno C, Gruenwald T, Haszpra**

568   **L**, **Hensen A**, **Ibrom A**, **Jacobs AFG**, **Jones MB**, **Lanigan G**, **Laurila T**, **Lohila**

569   **A**, **Manca G**, **Marcolla B**, **Nagy Z**, **Pilegaard K**, **Pinter K**, **Pio C**, **Raschim A**,

570   **Rogiers N**, **Sanz MJ**, **Stefanim P**, **Sutton M**, **Tuba Z**, **Valentini R**, **Williams ML**

571   and **Wohlfahrt G** (2007) Partitioning European grassland net ecosystem CO_2

572   exchange into gross primary productivity and ecosystem respiration using light

573   response function analysis. *Agriculture, Ecosystems & Environment*, **121**, 93–120.

574   **Giunta F**, **Pruneddu G** and **Motzo R** (2009) Radiation interception and biomass and

575   nitrogen accumulation in different cereal and grain legume species. *Field Crops*

576   *Research*, **110**, 76–84.

577   **Gliksman D, Navon Y, Dumbur, R. Haenel S, Grünzweig J** (2018) Higher rates of

578   decomposition in standing vs. surface litter in a Mediterranean ecosystem during

579   the dry and the wet seasons. *Plant Soil*, **428**, 427-439.

580   **Gomez-Casanovas N**, **Matamala R**, **Cook DR** and **Gonzalez-Meler MA** (2012) Net

581   ecosystem exchange modifies the relationship between the autotrophic and

582   heterotrophic components of soil respiration with abiotic factors in prairie

583   grasslands. *Global Change Biology*, **18**, 2532–2545.

584   **Groemping U** (2006) Relative Importance for Linear Regression in R: The Package

585   relaimpo. *Journal of Statistical Software*, **17**, 1–27.

586   **Hooper DU**, **Chapin FS**, **Ewel JJ**, **Hector A**, **Inchausti P**, **Lavorel S**, **Lodge DM**,

587   **Loreau M**, **Naeem S**, **Schmid B**, **Setälä H**, **Symstad AJ**, **Vandermeer J** and

588   **Wardle DA** (2005) Effects of Biodiversity on Ecosystem Functioning : A

589   Consensus of Current Knowledge. *Ecological Monographs*, **75**, 3–35.

590   **Imer D**, **Merbold L**, **Eugster W** and **Buchmann N** (2013) Temporal and spatial

591   variations of soil CO_2, CH_4 and N_2O fluxes at three differently managed grasslands.

592   *Biogeosciences*, **10**, 5931–5945.

593   **Kardol P**, **Cregger MA**, **Campany CE** and **Classen AT** (2010) Soil ecosystem

594   functioning under climate change: plant species and community effects. *Ecology*,

595   **91**, 767–781.

596   **Kirwan L**, **Lüscher A**, **Sebastià MT**, **Finn JA**, **Collins RP**, **Porqueddu C**,

597   **Helgadottir A**, **Baadshaug OH**, **Brophy C**, **Coran C**, **Dalmannsdóttir S**,

598   **Delgado I**, **Elgersma A**, **Fothergill M**, **Frankow-Lindberg BE**, **Golinski P**,

599   **Grieu P**, **Gustavsson AM**, **Höglind M**, **Huguenin-Elie O**, **Iliadis C**, **Jørgensen**

600   **M**, **Kadziuliene Z**, **Karyotis T**, **Lunnan T**, **Malengier M**, **Maltoni S**, **Meyer V**,

601   **Nyfeler D**, **Nykanen-Kurki P**, **Parente J**, **Smit HJ**, **Humm UT** and **Connolly J**

602   (2007) Evenness drives consistent diversity effects in intensive grassland systems

603   across 28 European sites. *Journal of Ecology*, **95**, 530–539.

604   **Lavorel S** and **Garnier E** (2002) Predicting changes in community composition and

605   ecosystem functioning from plant traits: revisiting the Holy Grail. *Functional*

606   *Ecology*, **16**, 545–556.

607   **Law BE**, **Falge E**, **Gu L**, **Baldocchi DD**, **Bakwin P**, **Berbigier P**, **Davis K**, **Dolman**

608   **AJ**, **Falk M**, **Fuentes JD**, **Goldstein A**, **Granier A**, **Grelle A**, **Hollinger D**,

609   **Janssens IA**, **Jarvis P**, **Jensen NO**, **Katul G**, **Mahli Y**, **Matteucci G**, **Meyers T**,

610   **Monson R**, **Munger W**, **Oechel W**, **Olson R**, **Pilegaard K**, **Paw U KT**,

611   **Thorgeirsson H**, **Valentini R**, **Verma S**, **Vesala T**, **Wilson K** and **Wofsy S** (2002)

612   Environmental controls over carbon dioxide and water vapor exchange of

613   terrestrial vegetation. *Agricultural and Forest Meteorology*, **113**, 97–120.

614   **Lee TD**, **Reich PB** and **Tjoelker MG** (2003) Legume presence increases

615   photosynthesis and N concentrations of co-occurring non-fixers but does not

616   modulate their responsiveness to carbon dioxide enrichment. *Oecologia*, **137**, 22–

617   31.

618   **Leifeld J**, **Meyer S**, **Budge K**, **Sebastia MT**, **Zimmermann M** and **Fuhrer J** (2015)

619   Turnover of grassland roots in mountain ecosystems revealed by their radiocarbon

620   signature: Role of temperature and management. *PLoS ONE*, **10**, 1–13.

621   **Leitinger G**, **Ruggenthaler R**, **Hammerle A**, **Lavorel S**, **Schirpke U**, **Clement J-C**,

622   **Lamarque P**, **Obojes N** and **Tappeiner U** (2015) Impact of droughts on water

623   provision in managed alpine grasslands in two climatically different regions of the

624   Alps. *Ecohydrology*, **8**, 1600–1613.

625   **Leitner S, Sae-Tun O, Kranzinger L, Zechmeister-Boltenstern S and Zimmermann**

626   **M** (2016) Contribution of litter layer to soil greenhouse gas emissions in a

627   temperate beech forest. *Plant Soil*, **403**, 455-469.

628   **Liu L, Liu L, Liang L, Donnelly A, Park I and Schwartz M** (2014) Effects o0f

629   elevation on spring phenological sensitivity to temperature in Tibetan Plateau

630   grasslands. *Chinese Science Bulletin*, **59**, 4856-4863.

631   **Metcalfe DB**, **Fisher RA** and **Wardle DA** (2011) Plant communities as drivers of soil

632   respiration: Pathways, mechanisms, and significance for global change.

633   *Biogeosciences*, **8**, 2047–2061.

634   **Minchin FR** and **Witty JF** (2005) Respiratory/Carbon Costs of Symbiotic Nitrogen

635   Fixation in Legumes. In *Plant Respiration. Advances in Photosynthesis and*

636   *Respiration, vol. 18* (Eds H. Lambers & M. Ribas-Carbo), pp. 195–205. Dordrecht:

637   Springer.

638   **Mitchell RM** and **Bakker JD** (2016) Grass abundance shapes trait distributions of

forbs in an experimental grassland. *Journal of Vegetation Science*, **27**, 557–567.

Moffat AM (2012) *A New Methodology to Interpret High Resolution Measurements of Net Carbon Fluxes between Terrestrial Ecosystems and the Atmosphere.* Ph.D. thesis, Friedrich-Schiller-Universität, Jena, Germany, 124 pp.

Nakano T and **Shinoda M** (2014) Modeling gross primary production and ecosystem respiration in a semiarid grassland of Mongolia. *Soil Science and Plant Nutrition*, **61**, 106–115.

Nyfeler D, **Huguenin-Elie O**, **Suter M**, **Frossard E**, **Connolly J** and **Lüscher A** (2009) Strong mixture effects among four species in fertilized agricultural grassland led to persistent and consistent transgressive overyielding. *Journal of Applied Ecology*, **46**, 683–691.

Nyfeler D, **Huguenin-Elie O**, **Suter M**, **Frossard E** and **Lüscher A** (2011) Grass-legume mixtures can yield more nitrogen than legume pure stands due to mutual stimulation of nitrogen uptake from symbiotic and non-symbiotic sources. *Agriculture, Ecosystems and Environment*, **140**, 155–163.

Pinheiro JC and **Bates DM** (2000) *Mixed-Effects Models in S and S-PLUS.* Springer New York.

Pinheiro JC, **Bates D**, **DebRoy S** and **Sarkar D** (2015) nlme: Linear and Nonlinear Mixed Effects Models. R package version 3.1-121.

Postgate J (1998) *Nitrogen Fixation*. Cambridge: Cambridge University Press.

Reich PB, **Buschena C**, **Tjoelker MG**, **Wrage K**, **Knops J**, **Tilman D** and **Machado JL** (2003) Variation in growth rate and ecophysiology among 34 grassland and savanna species under contrasting N supply: A test of functional group differences. *New Phytologist*, **157**, 617–631.

663 **Reich PB**, **Ellsworth DS** and **Walters MB** (1998) Leaf Structure (Specific Leaf Area)

664 Modulates Photosynthesis-Nitrogen relations: Evidence from within Across

665 Species and Functional Groups. *Functional Ecology*, **12**, 948–958.

666 **Reich PB**, **Walters MB** and **Ellsworth DS** (1997) From tropics to tundra: Global

667 convergence in plant functioning. *Ecology*, **94**, 13730–13734.

668 **Ribas A**, **Llurba R**, **Gouriveau F**, **Altimir N**, **Connolly J** and **Sebastià MT** (2015)

669 Plant identity and evenness affect yield and trace gas exchanges in forage mixtures.

670 *Plant Soil*, **391**, 93–108.

671 **Ryan MG** and **Law BE** (2005) Interpreting, measuring, and modeling soil respiration.

672 *Biogeochemistry*, **73**, 3–27.

673 **Schwinning S** and **Parsons AJ** (1996) Analysis of the coexistence mechanisms for

674 grasses and legumes in grazing systems. *Journal of Ecology*, **84**, 799–813.

675 **Sebastià M-T** (2007) Plant guilds drive biomass response to global warming and water

676 availability in subalpine grassland. *Journal of Applied Ecology*, **44**, 158–167.

677 **Silva JP**, **Toland J**, **Jones W**, **Eldridge J**, **Thorpe E** and **O'Hara E** (2008) *LIFE and*

678 *Europe′s Grasslands. Restoring a Forgotten Habitat* (Eds P. Owen, European

679 Commission, & Environment DG). Luxembourg: European Comission.

680 **Sjögersten S**, **Alewell C**, **Cecillon L**, **Hagedorn F**, **Jandl R**, **Leifeld J**, **Martinsen V**,

681 **Schindlbacher A**, **Sebastia MT** and **Van Miegroet H** (2011) Mountain soils in a

682 changing climate – vulnerability of carbon stocks and ecosystem feedbacks. In *Soil*

683 *Carbon in Sensitive European Ecosystems: From Science to Land Management*

684 (Eds R. Jandl, M. Rodeghiero, & M. Olsson), pp. 118–148.

685 **Sjögersten S**, **Llurba R**, **Ribas À**, **Yanez-Serrano A** and **Sebastià M-T** (2012)

686 Temperature and Moisture Controls of C Fluxes in Grazed Subalpine Grasslands.

687   *Arctic, Antarctic, and Alpine Research*, **44**, 239–246.

688   **Soussana JF**, **Allard V**, **Pilegaard K**, **Ambus P**, **Amman C**, **Campbell C**, **Ceschia E**,

689   **Clifton-Brown J**, **Czobel S**, **Domingues R**, **Flechard C**, **Fuhrer J**, **Hensen A**,

690   **Horvath L**, **Jones M**, **Kasper G**, **Martin C**, **Nagy Z**, **Neftel A**, **Raschi A**,

691   **Baronti S**, **Rees RM**, **Skiba U**, **Stefani P**, **Manca G**, **Sutton M**, **Tuba Z** and

692   **Valentini R** (2007) Full accounting of the greenhouse gas (CO_2, N_2O, CH_4) budget

693   of nine European grassland sites. *Agriculture, Ecosystems & Environment*, **121**,

694   121–134.

695   **Symstad AJ** (2000) A Test of the Effects of Functional Group Richness and

696   Composition on Grassland Invasibility. *Ecology*, **81**, 99–109.

697   **Thakur MP** and **Eisenhauer N** (2015) Plant community determines the strength of

698   top-down control in a soil food web motif. *Scientific Reports*, **5**, 1–6.

699   **Tilman D** (1997) Distinguishing between the effects of species diversity and species

700   composition. *Oikos*, **80**, 185.

701   **Tilman D**, **Lehman CL** and **Thomson KT** (1997) Plant diversity and ecosystem

702   productivity: Theoretical considerations. *Proceedings of the National Academy of*

703   *Sciences*, **94**, 1857–1861.

704   **Venables WN** and **Ripley BD** (2002) *Modern Applied Statistics with S*, 4th ed. New

705   York: Springer-Verlag New York.

706   **Wilson JB**, **Peet RK**, **Dengler J** and **Meelis P** (2012) Plant species richness: the world

707   records. *Journal of Vegetation Science*, **23**, 796–802.

708   **Wohlfahrt G**, **Anderson-Dunn M**, **Bahn M**, **Berninger F**, **Campbell C**, **Carrara A**,

709   **Cescatti A**, **Christensen T**, **Dore S**, **Friborg T**, **Furger M**, **Gianelle D**,

710   **Hargreaves K**, **Hari P**, **Haslwanter A**, **Marcolla B**, **Milford C**, **Nagy Z**, **Nemitz**

711   **E**, **Rogiers N**, **Sanz MJ**, **Siegwolf RTW**, **Susiluoto S**, **Sutton M**, **Tuba Z**, **Ugolini**

712   **F**, **Valentini R**, **Zorer R** and **Cernusca A** (2008a) Biotic, Abiotic, and

713   Management Controls on the Net Ecosystem CO_2 Exchange of European Mountain

714   Grassland Ecosystems. *Ecosystems*, **11**, 1338–1351.

715   **Wohlfahrt G**, **Hammerle A**, **Haslwanter A**, **Bahn M**, **Tappeiner U** and **Cernusca A**

716   (2008b) Disentangling leaf area and environmental effects on the response of the

717   net ecosystem CO_2 exchange to diffuse radiation. *Geophysical Research Letters*, **35**,

718   1–5.

719   **Wood SN** (2004) Stable and Efficient Multiple Smoothing Parameter Estimation for

720   Generalized Additive Models. *Journal of the American Statistical Association*, **99**,

721   673–686.

722   **Woodwell G** and **Whittaker R** (1968) Primary production in terrestrial ecosystems.

723   *American Zoologist*, **8**, 19–30.

724   **Wu Z**, **Dijkstra P**, **Koch GW**, **Peñuelas J** and **Hungate BA** (2011) Responses of

725   terrestrial ecosystems to temperature and precipitation change: a meta-analysis of

726   experimental manipulation. *Global Change Biology*, **17**, 927–942.

727   **Yvon-Durocher G**, **Caffrey JM**, **Cescatti A**, **Dossena M**, **Giorgio P**, **Gasol JM**,

728   **Montoya M**, **Pumpanen J**, **Staehr PA**, **Trimmer M**, **Woodward G** and **Allen AP**

729   (2012) Reconciling the temperature dependence of respiration across timescales

730   and ecosystem types. *Nature*, **487**, 472–476.

731   **Zhou J**, **Cai W**, **Qin Y**, **Lai L**, **Guan T**, **Zhang X**, **Jiang L**, **Du H**, **Yang D**, **Cong Z**

732   and **Zheng Y** (2016) Alpine vegetation phenology dynamic over 16 years and its

733   covariation with climate in a semi-arid region of China. *Science of the Total*

734   *Environment*, **572**, 119–128.

735   **Zuur AF**, **Ieno EN** and **Smith GM** (2007) *Analysing Ecological Data.* Springer New

736   York.

737

739   **Table 1.** CO_2 exchange linear model results: net ecosystem exchange (NEE), gross
740   primary production (GPP) and ecosystem respiration (R_{eco}), as function of aboveground
741   living biomass (AGLB), standing dead biomass (SDB), litter, air temperature (T_a), soil
742   water content (SWC) and site, with BERT as reference level. "Site x" indicates
743   interactions between site and the given variable. Estimates of the explanatory variables
744   (Est.), standard error (SE), t and P- value. Model adjusted R^2, degrees of freedom (DF)
745   and F-statistic.
746
747

|	NEE (μmol CO_2/m^2/s)				GPP (μmol CO_2/m^2/s)				R_{eco} (μmol CO_2/m^2/s)			
	Est.	SE	t	P	Est.	SE	t	P	Est.	SE	t	P
Intercept	−7	3.0	−2.46	0.02	4	6.0	0.60	0.6	−10	2.4	−4.01	< 0.001
AGLB	−0.05	0.010	−4.70	< 0.001	−0.06	0.012	−5.39	< 0.001	0.015	0.0035	4.37	< 0.001
SDB	0.019	0.0090	2.16	0.03	0.02	0.010	1.88	0.06				
Litter	0.05	0.020	2.30	0.02	0.04	0.022	1.63	0.1				
T_a	0.2	0.18	0.95	0.3	−0.5	0.25	−1.92	0.06	0.6	0.11	5.76	< 0.001
SWC					−36	17.3	−2.08	0.04	34	5.9	5.77	< 0.001
Site	27	8.3	3.23	0.002	29	9.9	2.92	0.005	1.5	0.88	1.75	0.08
Site x AGLB	0.03	0.016	1.83	0.07	0.04	0.018	2.01	0.05				
Site x litter	−0.08	0.027	−3.08	0.003	−0.07	0.030	−2.43	0.02				
Site x T_a	−1.7	0.62	−2.81	0.006	−2.1	0.71	−2.97	0.004				
R^2_{Adj}	0.53				0.6532				0.50			
DF	71				70				75			
F-statistic	12.05			< 0.001	17.53			< 0.001	20.37			<0.001

748

749 **Table 2.** Nonlinear mixed- effects models results, by the logistic sigmoid light response
750 function (Equation 3). Net ecosystem exchange (NEE) as a function of
751 photosynthetically active radiation (PAR): (1) NEE ~ PAR per grassland ground area
752 (NEE, µmol CO_2/m²/s) and (2) NEE normalized by living biomass (NEE_{AGLB}, µmol
753 CO_2/g/s). Model 1.1 and 2.1 (null models), parameters as fixed effects: quantum yield
754 (α), asymptotic gross primary production (GPP_{sat}) and daytime ecosystem respiration
755 ($R_{eco,day}$). Models 1.2 and 2.2 plant functional type (PFT) dominance as covariates. PFT
756 dominance with L- dominated as reference level. Estimates (Est.), standard error (SE), t
757 and P- value. Model R^2, degrees of freedom (DF) and ANOVAs comparing models.

758

759

		Parameter	Est.	SE	t	P	DF	R^2
Model 1.1 **NEE ~ PAR**	**α**	Intercept	0.035	0.0060	5.83	< 0.001		
	GPP$_{sat}$	Intercept	28	3.5	7.92	< 0.001	117	0.69
	R$_{eco,day}$	Intercept	10	1.6	6.12	< 0.001		
Model 1.2 **NEE ~ PAR +** **PFT**	**α**	Intercept	0.025	0.0085	3.00	0.003		
		F-dominated	0.00	0.011	0.20	0.8		
		G-dominated	0.02	0.016	1.44	0.2		
	GPP$_{sat}$	Intercept	25	3.7	6.76	< 0.001	111	0.68
		F-dominated	6	5.6	1.03	0.3		
		G-dominated	6	4.8	1.31	0.2		
	R$_{eco.day}$	Intercept	7	2.8	2.45	0.02		
		F-dominated	1	3.6	0.41	0.7		
		G-dominated	7	4.1	1.73	0.1		
ANOVA model 1.1 vs. 1.2						0.97		
Model 2.1 **NEE$_{AGLB}$ ~ PAR**	**α**	Intercept	0.00013	0.000038	3.47	0.0007		
	GPP$_{sat}$	Intercept	0.12	0.011	10.26	< 0.001	117	0.66
	R$_{eco,day}$	Intercept	0.037	0.0085	4.34	< 0.001		
Model 2.2 **NEE$_{AGLB}$ ~ PAR +** **PFT**	**α**	Intercept	0.00012	0.000041	2.97	0.004		
		F-dominated	0.00003	0.000042	0.64	0.5		
		G-dominated	0.00002	0.000067	0.35	0.7		
	GPP$_{sat}$	Intercept	0.14	0.019	7.43	< 0.001	111	0.72
		F-dominated	−0.02	0.022	−1.10	0.3		
		G-dominated	−0.05	0.022	−2.29	0.02		
	R$_{eco.day}$	Intercept	0.03	0.012	2.58	0.01		
		F-dominated	0.01	0.014	0.68	0.5		
		G-dominated	0.01	0.016	0.64	0.5		
ANOVA model 2.1 vs. 2.2						0.001		

762
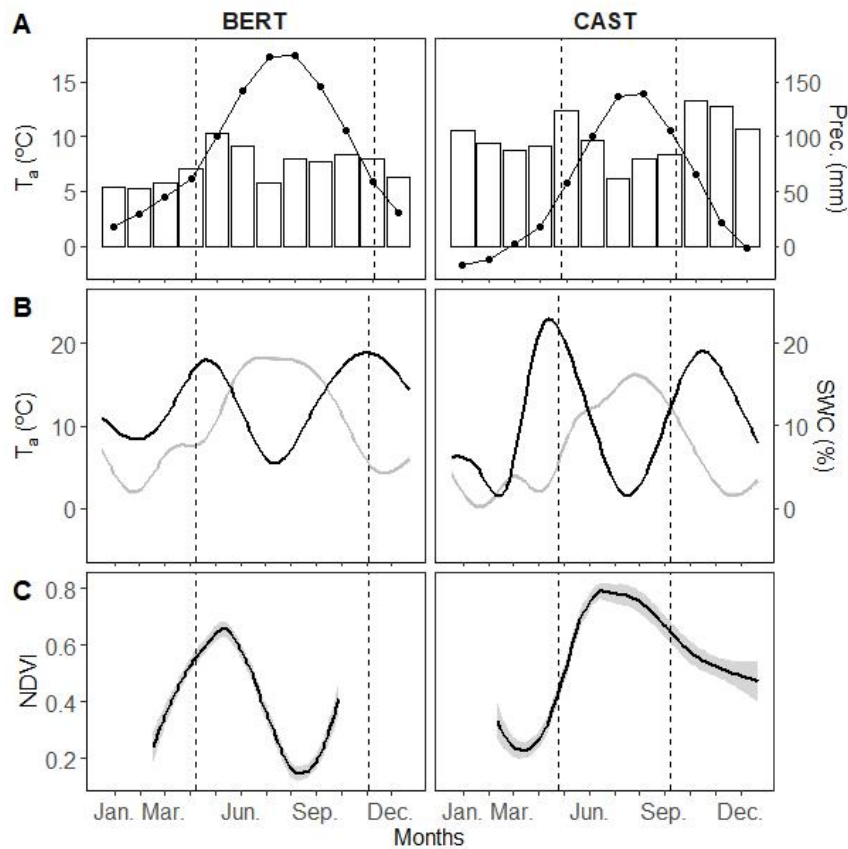
Figure 1. Climatic and environmental variables of the study sites: Bertolina (BERT) and Castellar (CAST). (A) Mean climatic (1970–2000) monthly air temperature (T_a, solid symbols and line) and monthly precipitation (bars), source: WorldClim (Fick & Hijmans 2017); (B) 2012 meteorological data: T_a (grey line), and soil water content at 5 cm depth (SWC, black line), lines fitted using generalized additive models with integrated smoothness estimation (gam), mgcv package (Wood 2004), source: eddy covariance flux stations; (C) 2012 normalized difference vegetation index (NDVI, black line) and its 0.95 confidence interval (grey band), line fitted using local polynomial regression fitting (loess), source: eddy covariance flux stations. Vertical black dashed lines indicate the beginning and the end of the study period.

773

774
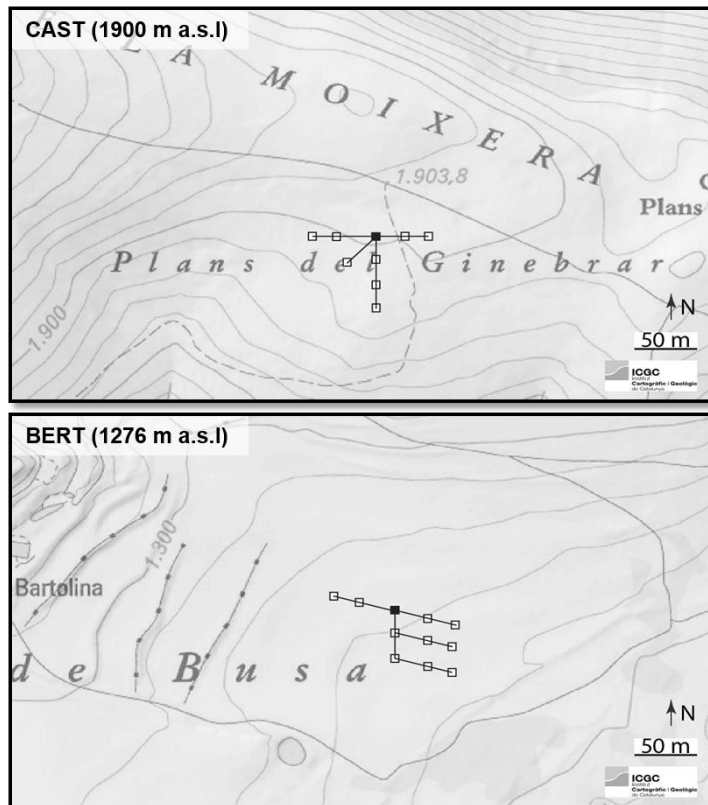
Figure 2. Map of the study sites, Bertolina (BERT) and Castellar (CAST), and scheme of the seasonal sampling design. White blocks: sampling points, black blocks: eddy covariance stations. Every sampling day new sampling points were selected. Contour line interval 10 m.

779

780
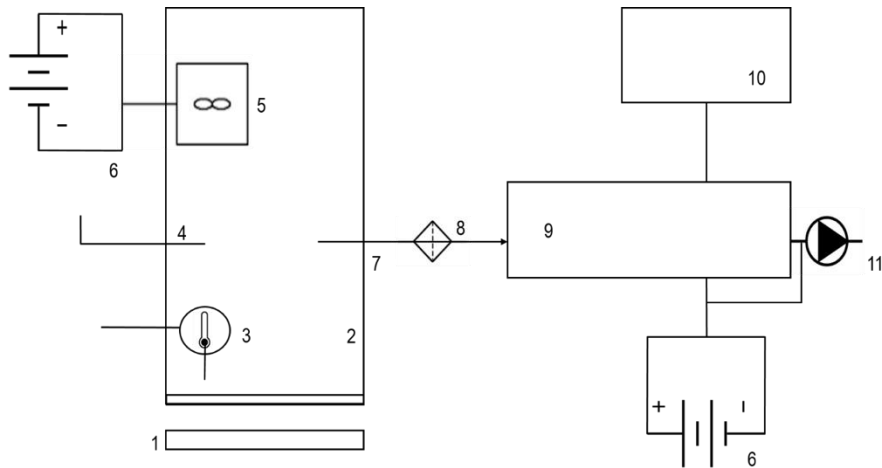
Figure 3. Scheme of the gas-exchange measurement system set-up. (1) metal collars (height = 8 cm, inner diameter = 25 cm), hammered into the soil around three weeks before to let the system recover from the disturbance; (2) methacrylate chamber (height = 38.5 cm, inner diameter = 25 cm), rubber joint at its base to provide sealing at the chamber- ring junction; (3) multi-logger thermometer (TMD-56, Amprove, USA); (4) vent to avoid underpressure inside the chamber (Davidson *et al*. 2002); (5) fan to homogenize the air in the headspace; (6) batteries; (7) polyethylene liner with ethyl vinyl acetate shell tube (Bev a Line IV, longitude = 15.3 m, inner diameter = 3.175 mm); (8) air filter (pore size = 0.1 μm); (9) infrared gas analyser (LI-840, LI-COR, USA); (10) laptop and (11) air pump, output flow set at $1.67 \cdot 10^{-5}$ m^3/s, which is 1 litres/min.

792
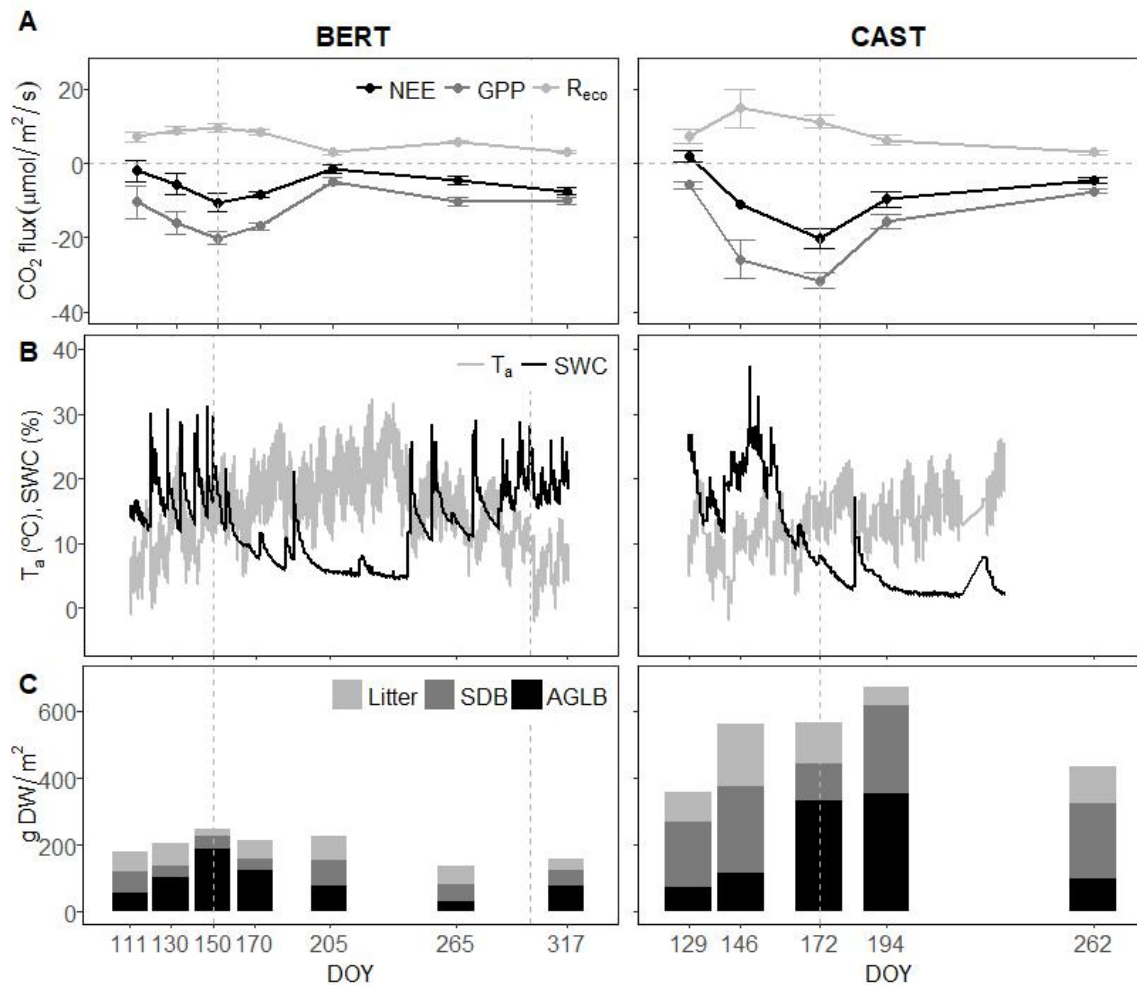
Figure 4. Seasonal dynamics (DOY: day of year): (A) Mean daytime CO_2 exchange fluxes: net ecosystem exchange (NEE), gross primary production (GPP) and ecosystem respiration (R_{eco}) ± standard error; (B) 30 min. averaged air temperature (T_a) and volumetric soil water content (SWC) at 5 cm depth, source: eddy covariance stations. A system failure of the eddy covariance flux station at CAST caused missing meteorological data from DOY 219 up to the end of the study period; (C) mean litter, standing dead biomass (SDB) and aboveground living biomass (AGLB). Grey dashed vertical lines indicate the beginning and end of the grazing period.
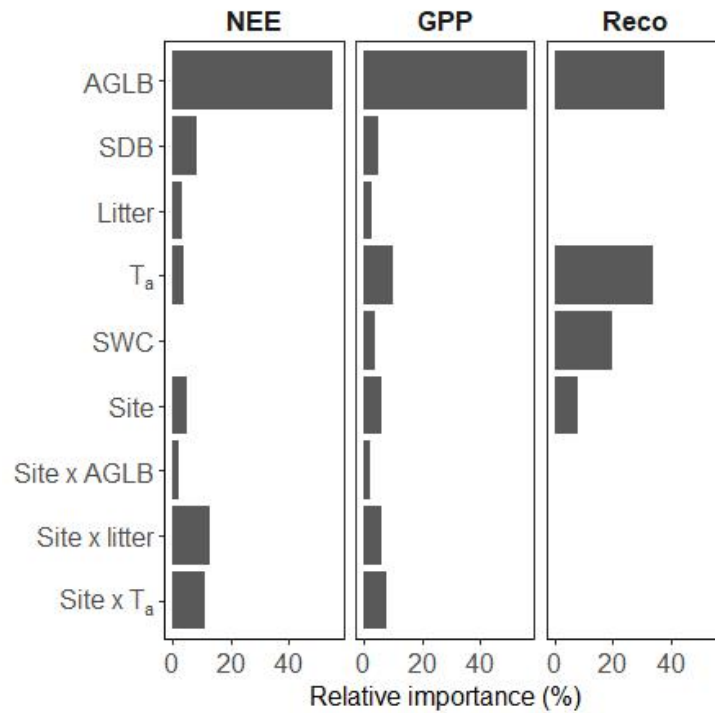
804

805

806 **Figure 5.** Relative importance of explicative variables linear modelling (Table 1):
807 aboveground living biomass (AGLB), standing dead biomass (SDB), litter, air
808 temperature (T_a), soil water content (SWC) and site, with BERT as reference level. "Site
809 x" indicates interactions between site and the given variable.

according to the linear model (Table 1).
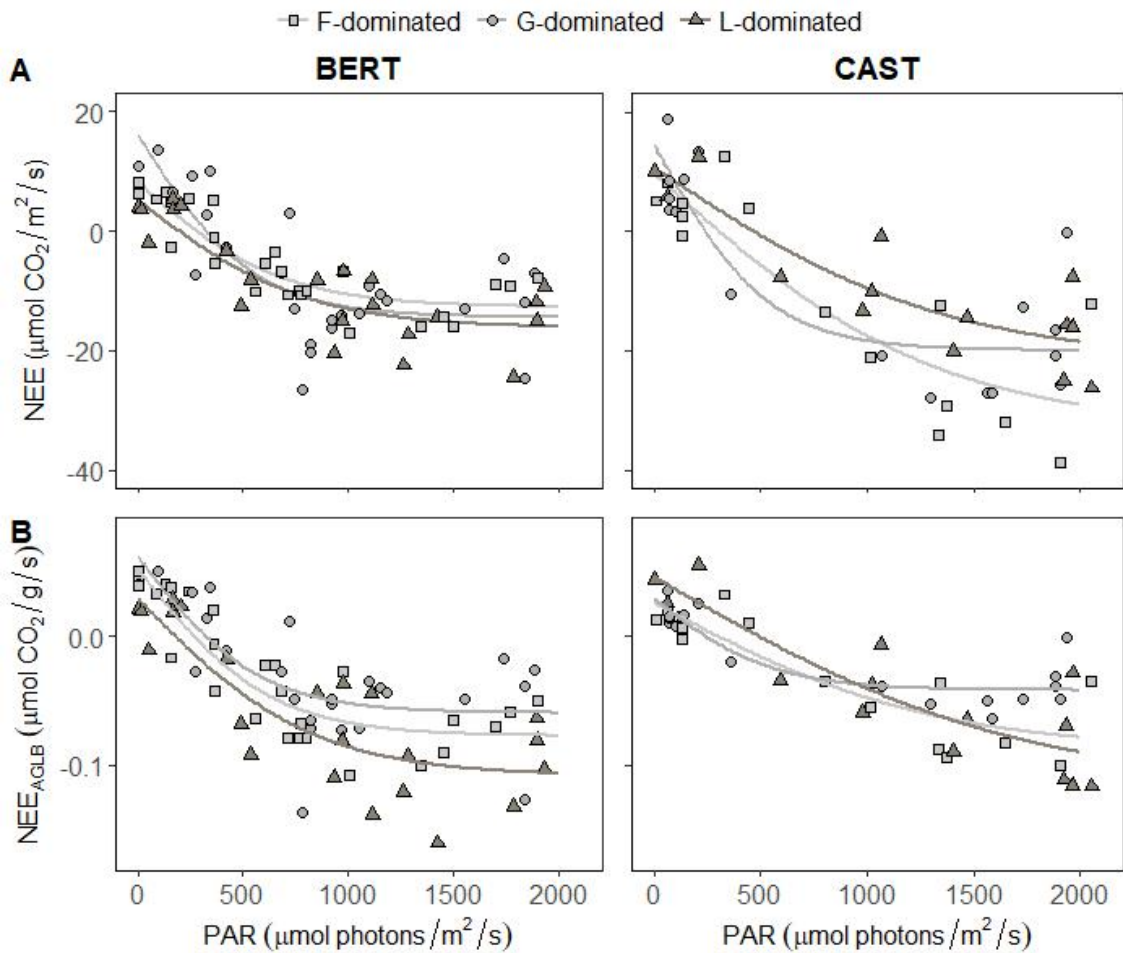
Figure 6. Observed NEE (points) vs. predicted NEE (line) by the logistic sigmoid light response function (Equation 3) per site and per plant functional type (PFT) dominance — forbs dominated (F- dominated), grasses dominated (G- dominated), and legumes dominated (L- dominated) — based on (A) NEE per unit of grassland ground area (NEE μmol $CO_2/m^2/s$) and (B) NEE per unit of aboveground living biomass (NEE$_{AGLB}$ μmol $CO_2/g/s$).
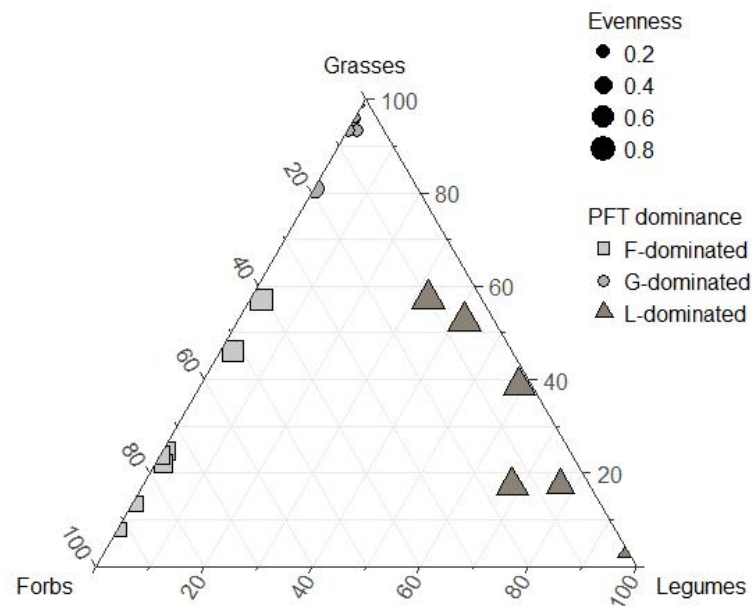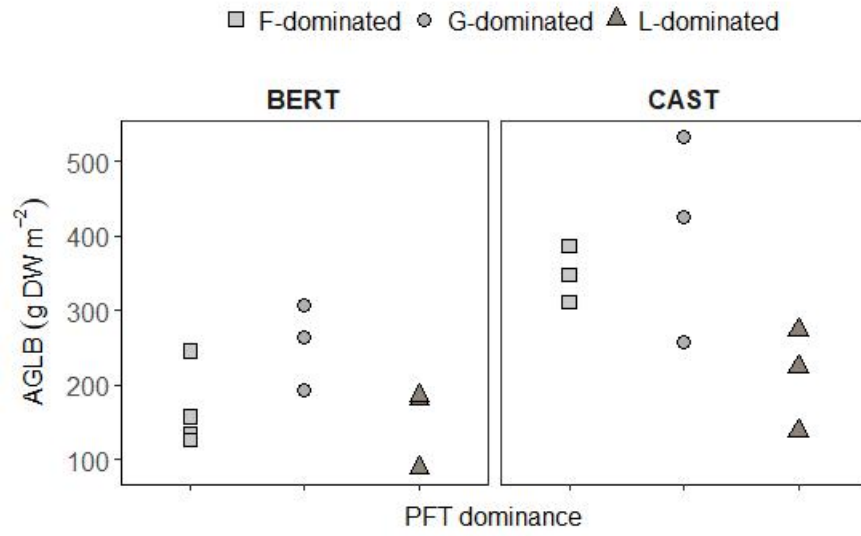
Supplementary material

Figure S1. Plant functional type (PFT) dominance groups — forbs dominated (F‑dominated), grasses dominated (G‑dominated), and legumes dominated (L‑dominated) — after clustering (Ward's method), based in the proportion of each PFT and the evenness index (Kirwan *et al.* 2007). The position in the ternary plot indicates the proportion of the corresponding PFT and the size of the point corresponds to the evenness index.

Figure S2. Aboveground living biomass (AGLB) per site and per plan functional type (PFT) dominance group: forbs dominated (F-dominated), grasses dominated (G- dominated) and legumes dominated (L-dominated).